

Resonant excitation of Er^{3+} by the energy transfer from Si nanocrystals

Kei Watanabe

Graduate School of Science and Technology, Kobe University, Rokkodai, Nada, Kobe 657-8501, Japan

Minoru Fujii^{a)} and Shinji Hayashi

Department of Electrical and Electronics Engineering, Faculty of Engineering, Kobe University, Rokkodai, Nada, Kobe 657-8501, Japan

(Received 2 October 2000; accepted for publication 13 August 2001)

Photoluminescence (PL) properties of SiO_2 films containing Si nanocrystals (*nc*-Si) and Er were studied. The average size of *nc*-Si was changed in a wide range in order to tune the exciton energy of *nc*-Si to the energy separations between the discrete electronic states of Er^{3+} . PL from exciton recombination in *nc*-Si and the intra-4*f* shell transition of Er^{3+} were observed simultaneously. At low temperatures, periodic features were observed in the PL spectrum of *nc*-Si. The period agreed well with the optical phonon energy of Si. The appearance of the phonon structure implies that *nc*-Si which satisfy the energy conservation rule during the energy transfer process can resonantly excite Er^{3+} . For the PL from Er^{3+} , a delay was observed after the pulsed excitation of *nc*-Si hosts. The rise time of the PL showed strong size dependence. The effects of the quantum confinement of excitons in *nc*-Si on the energy transfer process are discussed. © 2001 American Institute of Physics. [DOI: 10.1063/1.1409572]

I. INTRODUCTION

Recently, Er-doped Si has been attracting a lot of attention, because Er^{3+} ions incorporated into Si produce stable sharp luminescence from the intra-4*f* shell transition ($^4I_{13/2}$ to $^4I_{15/2}$) at around 0.81 eV, which corresponds to the absorption minimum in silica-based glass fibers. Electroluminescence devices operating at room temperature have been realized,¹⁻⁵ and many attempts have been made to improve the quantum efficiency. The excitation mechanism of Er^{3+} in a bulk-Si crystal is generally explained as follows.⁵ First, an electron-hole pair generated in Si is trapped at an Er-related level about 0.15 eV below the bottom of the conduction band. The recombination energy of the trapped electron-hole pair is then transferred to Er^{3+} (energy transfer), and the 4*f* shell is excited. A drawback to use a bulk Si crystal as a host of Er^{3+} is the large temperature quenching of the 0.81 eV luminescence. The temperature quenching arises from the dissociation of an electron-hole pair bound to the Er-related level before the energy is transferred to Er^{3+} and the de-excitation of an excited Er^{3+} by forming an electron-hole pair at the Er-related level (energy back transfer).⁵⁻⁸ The temperature quenching can drastically be reduced by using Si nanostructures such as porous Si and Si nanocrystals (*nc*-Si) as a host of Er.^{5,9-19} The band gap widening of Si nanostructures arising from the confinement of an electron-hole pair in a small volume (quantum size effects) is considered to be responsible for the observed small temperature quenching.

In our previous work,¹²⁻¹⁴ we have studied photoluminescence (PL) from SiO_2 films containing *nc*-Si and Er and discussed the excitation mechanism of Er^{3+} via *nc*-Si. The

samples exhibited strong 0.81 eV PL at room temperature as well as 1.5 eV PL due to the recombination of excitons in *nc*-Si. The correlation between the intensities of the two PL peaks was studied. We found that the 0.81 eV peak becomes strong as the Er concentration increases, while the 1.5 eV peak becomes weak. These results combined with the excitation spectra of the two PL peaks suggest that the excitation of Er^{3+} is made by the energy transfer from *nc*-Si.

The energy transfer process has been discussed in detail on the basis of the time kinetics of the PL bands and rate equations, and some different models are proposed.^{16,17,19,20} However, no spectroscopic evidences which indicate the strong coupling between *nc*-Si and Er^{3+} have been obtained. Since the electronic states of Er^{3+} are discrete and the band gap of *nc*-Si changes with the size, *nc*-Si with some specific sizes can resonantly excite Er^{3+} . Observation of such resonant nature offers direct evidence of the energy coupling and gives useful information to understand the energy transfer mechanism. Furthermore, the energy transfer rate has not been estimated; it is not known whether or not the energy transfer rate depends on the size. Since the energy transfer rate is an important parameter which determines the luminescence efficiency, an estimation of the rate and the evaluation of the size dependence is indispensable to fully understand the energy transfer mechanism and to further improve the luminescence efficiency of Er-doped Si nanostructures.

In this work, we studied PL and PL decay dynamics of SiO_2 films containing *nc*-Si and Er. The average size of *nc*-Si was changed in a wide range in order to tune the exciton energy of *nc*-Si to the energy separations between the discrete electronic states of Er^{3+} . This wide tunability provides valuable information to understand the energy transfer mechanism. We will demonstrate that phonon-related periodic features appear on the PL spectra of *nc*-Si. The appearance of the features implies the existence of a

^{a)}Author to whom correspondence should be addressed; electronic mail: fujii@eedept.kobe-u.ac.jp

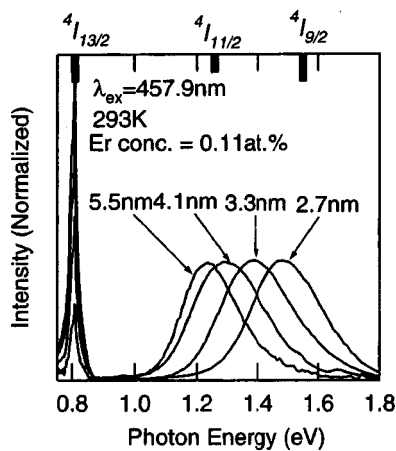


FIG. 1. PL spectra of SiO_2 films containing nc -Si and Er at room temperature. The size of nc -Si is varied from 2.7 to 5.5 nm, and the Er concentration (C_{Er}) is fixed at 0.11 at. %. The energy position of the first (${}^4I_{13/2}$), second (${}^4I_{11/2}$), and third (${}^4I_{9/2}$) excited states of Er^{3+} measured from the ground state is shown.

resonant energy transfer process. We will also show that the $4f$ shell PL of Er^{3+} exhibits a delay after the pulsed excitation of nc -Si hosts, and the rise time depends strongly on the size of nc -Si. The effects of the quantum confinement of excitons in nc -Si on the efficient PL of Er^{3+} are discussed.

II. EXPERIMENT

SiO_2 films containing nc -Si and Er were prepared by a co-sputtering method. Details of the preparation procedures are described in our previous papers.^{12,13} In this work, the average size of nc -Si (d_{Si}) was changed from 2.7 to 5.5 nm. PL spectra were measured using a single grating monochromator and a near-infrared photomultiplier with a InP/InGaAs photocathode. This near-infrared-sensitive fast photomultiplier allows us to measure time response of PL from Er^{3+} with the time resolution of less than 10 ns. The excitation source was the 457.9 nm line of an Ar-ion laser. For all the spectra, the spectral response of the detection system was corrected by the reference spectrum of a standard tungsten lamp. For the time response measurements, the 532.0 nm line of a Nd:yttrium-aluminum-garnet laser was used as an excitation source. The pulse width was 5 ns and the repetition frequency was 20 Hz. A multichannel scalar was used in obtaining decay curves. The time resolution of the system was about 40 ns.

III. RESULTS

A. PL spectra

Figure 1 shows PL spectra at room temperature. All the samples show two peaks. The low-energy one (0.81 eV) corresponds to the intra- $4f$ shell transition of Er^{3+} (${}^4I_{13/2}$ to ${}^4I_{15/2}$) (Er^{3+} PL),⁵ while the high-energy one to the recombination of excitons confined in nc -Si (nc -Si PL).^{12,13,21} The PL from nc -Si depends strongly on the size. The PL peak is shifted from 1.2 to 1.5 eV as the size decreases from 5.5 to 2.7 nm. Although not shown here, the intensity ratio of the two PL peaks depends strongly on the Er concentration and

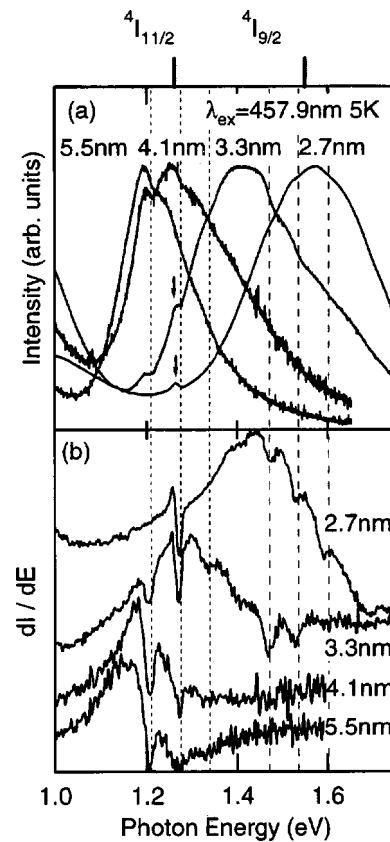


FIG. 2. (a) PL spectra in the range between 1.0 and 1.75 eV at 5 K and (b) the first derivative. Vertical lines are drawn with the period of 64 meV. The energy position of the second (${}^4I_{11/2}$) and third (${}^4I_{9/2}$) excited states of Er^{3+} measured from the ground state is shown.

the excitation power.¹² The Er^{3+} PL becomes intense with Er concentration, while the nc -Si one becomes weak.

Figure 2(a) shows the PL spectra at 5 K. Only the spectral range between 1.0 and 1.75 eV is shown. In contrast to the featureless spectral shape at room temperature, periodic features can clearly be distinguished, i.e., the spectra are periodically suppressed, and dips appear periodically. In particular, for the sample with $d_{\text{Si}}=5.5$ nm, the higher energy part of the spectrum is strongly suppressed. It should be noted here that without Er doping, the spectra are featureless even at 5 K. The first derivatives of the spectra are shown in Fig. 2(b). In all the spectra, the features in the derivative spectra appear at the same energy. The energy separations between the three features in the low-energy side as well as those in the high-energy side are almost the same. The vertical lines are drawn at every 64 meV, and correspond well to the features in the derivative spectra. Besides periodic dips, a small peak is seen at 1.26 eV (indicated by arrows). This peak is due to the transition between the second excited (${}^4I_{11/2}$) and ground states (${}^4I_{15/2}$) of Er^{3+} . This peak is observed only when relatively small nc -Si are co-doped, i.e., when the PL energy of nc -Si is larger than the energy separation between the third excited state (${}^4I_{9/2}$) and the ground state (${}^4I_{15/2}$).

B. PL decay dynamics

Figure 3(a) shows the nc -Si PL decay curves detected at the maximum of nc -Si PL in Fig. 1 at room temperature. The

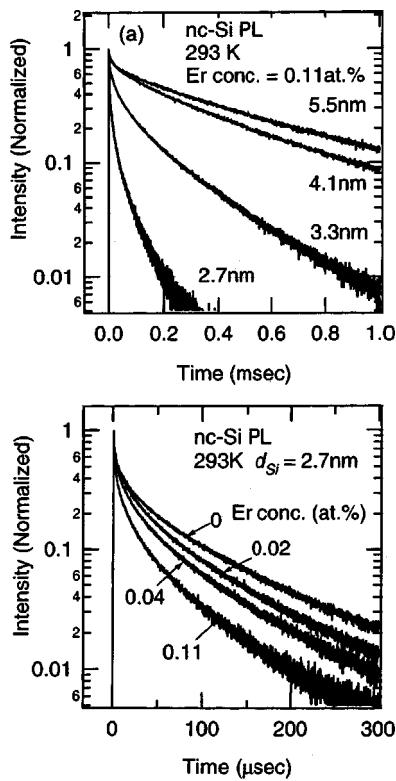


FIG. 3. (a) Decay curves of photoluminescence from *nc*-Si measured at the maximum of the spectra in Fig. 1. (b) Er concentration dependence of the decay curves for the sample with $d_{Si}=2.7$ nm. The Er concentration is varied from 0 to 0.11 at. %.

decay curves are nonexponential. The PL lifetime becomes shorter as the size decreases. Figure 3(b) shows Er concentration dependence of the *nc*-Si PL decay curves for the sample with $d_{Si}=2.7$ nm. As the Er concentration increases, the lifetime becomes shorter. The decay curves were well fitted by the modified stretched exponential function, which is generally used to analyze the decay curves of porous Si.²² The lifetime obtained for the sample not containing Er is about 79 μ s, while that for the sample with the largest Er concentration is about 47 μ s. The shortening of the lifetime of the host (*nc*-Si) PL with increasing Er concentration implies that the energy transfer is mediated by photogenerated excitons, i.e., not due to the absorption of light emitted by *nc*-Si. In other words, energy transfer to Er^{3+} is a preferential nonradiative recombination channel for *nc*-Si. As will be discussed later, the shortening of the lifetime is mainly due to “nonresonant” energy transfer. The contribution of “resonant” energy transfer is rather small.

In Fig. 3(b), the reduction of the decay time by Er doping is rather small. It is worth nothing that the small reduction does not mean that the energy transfer to Er occurs on a timescale similar to that of the radiative exciton recombination process. If the decay curve reflects only the radiative exciton recombination process, this argument seems to be correct. However, PL decay curves of pure *nc*-Si in Fig. 3 reflect not only the radiative exciton recombination process but also non-radiative recombination processes. Therefore, only from the *nc*-Si decay curves, the timescale of the energy transfer cannot simply be discussed. As will be shown later, the energy transfer time can be estimated from PL rise time,

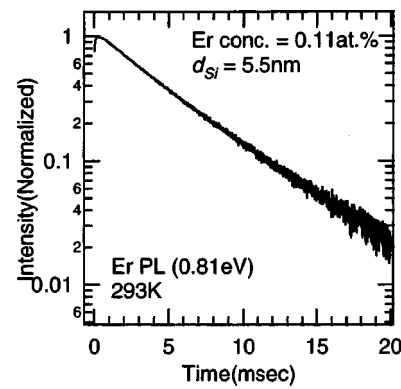


FIG. 4. A typical decay curve of Er^{3+} PL. The decay curve did not strongly depend on Er concentration.

and is much shorter than the estimated radiative exciton recombination time even at room temperature.

In previous PL studies of similar samples, the decay time of *nc*-Si PL was reported to be insensitive to Er concentration.^{17,18} The reason for this contradiction is not clear at present. However, we measured *nc*-Si PL decay curves for several series of samples, and the shortening of the lifetime with increasing Er concentration was observed for all the series.

The Er^{3+} PL decay curve detected at 0.81 eV is shown in Fig. 4 for the sample with $d_{Si}=5.5$ nm. The lifetime is about 5 ms. The lifetime became slightly long with decreasing the size (as listed in Table I). However, it is not clear whether it is really a size effect or it is related to sample preparation parameters, e.g., Si concentration and annealing temperature, which are changed to control the size. The lifetime was almost independent of the Er concentration.

The Er^{3+} PL decay curves at 0.81 eV immediately after pulsed excitation of *nc*-Si hosts are shown in Fig. 5. The pulse width is 5 ns. We can clearly see the PL delay for all samples. The PL delay becomes remarkable as the size of *nc*-Si increases. We roughly estimated the rise time τ_{rise} by the following procedure. The slow decay part (400μ s $< t < 1$ ms) of the data was first fitted by a single exponential function, and then the fitted function is subtracted from the experimental decay curve. The resultant data were not a single-exponential function. We thus tried to fit the curve again by a stretched exponential function, $I_{Er}(t) = 1 - I_o \exp\{-t/(\tau_{rise})\}^\beta$. The data could be well fitted by the function. Although there is no theoretical model which indicates that the rising part will be a stretched-exponential function, it is convenient to quantitatively estimate the size dependence of the rise time. The possible reason for the deviation of the rising part from a single-exponential func-

TABLE I. Radiative recombination time of excitons in *nc*-Si (τ_R), lifetime of the lowest excited state of Er^{3+} (τ_{Er}), rise time of Er^{3+} PL after pulsed excitation of *nc*-Si hosts (τ_{rise}), and energy transfer time (τ_{Tr}).

d_{Si} (nm)	τ_R (μ s)	τ_{Er} (μ s)	τ_{rise} (μ s)	τ_{Tr} (μ s)
2.7	107	7100	4.1	11
3.3	298	5800	6.4	21
4.1	747	5500	11	39
5.5	990	5000	38	115

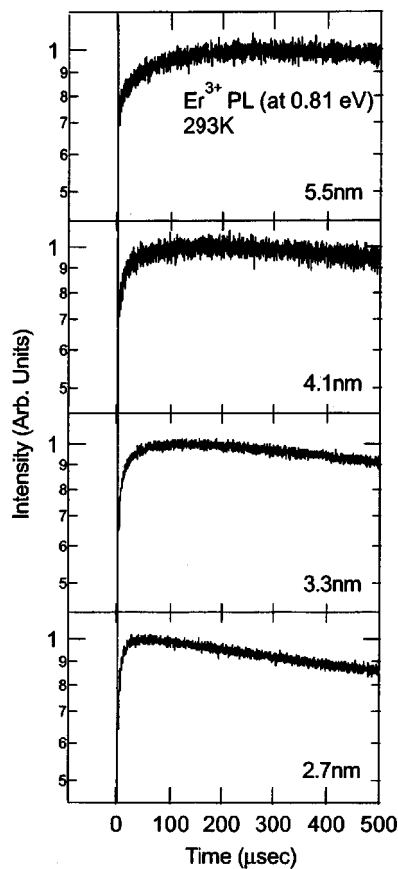


FIG. 5. Decay curves of Er^{3+} PL just after the pulsed excitation of $nc\text{-Si}$ hosts. The size of $nc\text{-Si}$ is varied from 2.7 to 5.5 nm and the Er concentration is fixed at 0.11 at. %.

tion will be discussed in the next subsection. The estimated values of τ_{rise} are listed in Table I.

The PL delay was observed for all the samples containing both $nc\text{-Si}$ and Er. Within the present sample preparation condition, the delay time depended only on the size of $nc\text{-Si}$, but did not depend on the Er concentration. This Er concentration insensitiveness seems to suggest that, on average, each nanocrystal can interact with less than one Er^{3+} even in the sample with the highest Er concentration. If Er concentration is further increased, the number of Er^{3+} which can interact with one nanocrystal will exceed one. This might change the properties of the interaction, and the effect should appear on the rise time. Detailed theoretical consideration is required to further discuss this problem. However, this is out of the scope of this article.

In all the spectra, we can see a very fast component after the pulsed excitation; this component is faster than the system response time. The component was observed for the sample not containing Er, suggesting that the component is not related to Er and is a background signal. A very similar fast decay component was observed for the PL decay curve of Er-doped bulk Si,⁸ but the origin of the fast component was not identified.

C. Analysis of the PL decay curves

Here, we analyze the observed PL decay curves. The time evolution of Er^{3+} luminescence is a very complicated

process.²³ In the following discussion, to simplify the problem and to extract important parameters from the observed decay curves, we will make the following assumptions: (i) excitation pulse is so short that no energy transfer occurs during the pulsed excitation, (ii) excitation pulse is so weak that most of the Er atoms are not directly excited, (iii) that nonlinear effects do not occur in $nc\text{-Si}$, and (iv) there is no energy back transfer process. The first assumption is valid because the pulse width (5 ns) is apparently much shorter than the observed PL delay. The second assumption is also valid because in the same experimental condition Er^{3+} PL was not observed for the sample not containing $nc\text{-Si}$. Furthermore, the intensity of $nc\text{-Si}$ PL was in proportion to the excitation power. The last assumption is also possible, because we observed almost no temperature quenching of Er^{3+} PL.

In the present samples, $nc\text{-Si}$ are isolated from the others by SiO_2 barriers 4–5 nm in thickness.²⁴ Thus, diffusion of carriers between $nc\text{-Si}$ does not occur. In this situation, $nc\text{-Si}$ can be classified into two categories, i.e., $nc\text{-Si}$ with no nonradiative centers and those with at least one such center. The PL lifetime of the former $nc\text{-Si}$ is equal to the radiative recombination time (τ_R) of excitons in $nc\text{-Si}$, while that of the latter one is expressed as $1/(1/\tau_R + 1/\tau_{\text{NR}})$, where τ_{NR} is the lifetime of nonradiative recombination of excitons in $nc\text{-Si}$ and is generally much smaller than τ_R . The number of excited $nc\text{-Si}$ having no nonradiative recombination centers [$N_{\text{Si-R}}(t)$] and that having nonradiative recombination centers [$N_{\text{Si-NR}}(t)$] can be expressed as

$$N_{\text{Si-R}}(t) = N_{\text{Si-R}}^0 \exp\left\{-\left(\frac{1}{\tau_R}\right)t\right\}, \quad (1)$$

$$N_{\text{Si-NR}}(t) = N_{\text{Si-NR}}^0 \exp\left\{-\left(\frac{1}{\tau_R} + \frac{1}{\tau_{\text{NR}}}\right)t\right\}, \quad (2)$$

where $N_{\text{Si-R}}^0$ and $N_{\text{Si-NR}}^0$ are the number of excited $nc\text{-Si}$ at $t=0$. The $nc\text{-Si}$ PL intensity is

$$I_{\text{Si}}(t) \propto -\frac{\delta}{\delta t} \left[N_{\text{Si-R}}(t) + \frac{1/\tau_R}{1/\tau_R + 1/\tau_{\text{NR}}} N_{\text{Si-NR}}(t) \right], \quad (3)$$

$$\propto \frac{1}{N_{\text{Si-R}}^0 + \left(\frac{1/\tau_R}{1/\tau_R + 1/\tau_{\text{NR}}}\right) N_{\text{Si-NR}}^0} \left[N_{\text{Si-R}}^0 \exp\left\{-\left(\frac{1}{\tau_R}\right)t\right\} + N_{\text{Si-NR}}^0 \exp\left\{-\left(\frac{1}{\tau_R} + \frac{1}{\tau_{\text{NR}}}\right)t\right\} \right]. \quad (4)$$

In Er-doped samples, a new nonradiative recombination process, i.e., the energy transfer process, should be added. The energy transfer time (τ_{Tr}) is considered to be much larger than τ_{NR} , because the sum of the intensities of the two PL peaks ($nc\text{-Si}$ PL and Er^{3+} PL) is almost independent of Er concentration; if $\tau_{\text{Tr}} \leq \tau_{\text{NR}}$, the total intensity should increase with Er concentration. Furthermore, τ_{Tr} is smaller than τ_R , because the energy transfer is the preferential recombination channel for excitons in Si nanocrystals. Therefore, the following relation holds between the three parameters:

$$\tau_{NR} \ll \tau_{Tr} < \tau_R. \tag{5}$$

Equation (5) indicates that *nc*-Si which originally do not have nonradiative recombination centers can transfer energy to Er, and those having nonradiative recombination centers do not participate in the energy transfer process. Under this simple approximation, the number of excited *nc*-Si which shows exciton recombination PL [$N_{Si-R}(t)$] and which can transfer energy to Er^{3+} [$N_{Si-Er}(t)$] can be expressed as

$$N_{Si-R}(t) = (N_{Si-R}^0 - N_{Si-Er}^0) \exp\left\{-\left(\frac{1}{\tau_R}\right)t\right\}, \tag{6}$$

$$N_{Si-Er}(t) = N_{Si-Er}^0 \exp\left\{-\left(\frac{1}{\tau_R} + \frac{1}{\tau_{Tr}}\right)t\right\}, \tag{7}$$

where N_{Si-Er}^0 is the number of excited *nc*-Si which will transfer energy to Er^{3+} . The *nc*-Si PL intensity is

$$I_{Si}(t) \propto \frac{1}{(N_{Si-R}^0 - N_{Si-Er}^0) + \left(\frac{1/\tau_R}{1/\tau_R + 1/\tau_{Tr}}\right)N_{Si-Er}^0 + \left(\frac{1/\tau_R}{1/\tau_{Tr} + 1/\tau_{NR}}\right)N_{Si-NR}^0} \times \left[(N_{Si-R}^0 - N_{Si-Er}^0) \exp\left\{-\left(\frac{1}{\tau_R}\right)t\right\} + N_{Si-Er}^0 \exp\left\{-\left(\frac{1}{\tau_R} + \frac{1}{\tau_{Tr}}\right)t\right\} + N_{Si-NR}^0 \exp\left\{-\left(\frac{1}{\tau_R} + \frac{1}{\tau_{NR}}\right)t\right\} \right]. \tag{8}$$

In this equation, we can see that, with increasing Er concentration, the contribution of the second term increases, resulting in the shortening of the *nc*-Si PL lifetime. This is consistent with the experimental results shown in Fig. 3(b). In Eq. (8), only the second term is related to the excitation process of Er^{3+} . If one *nc*-Si excites one Er^{3+} , the number of excited Er^{3+} will be

$$N_{Er}(t) = [N_{Si-Er}^0 - N_{Si-Er}(t)] \exp\left\{-\left(\frac{1}{\tau_{Er}}\right)t\right\}, \tag{9}$$

where τ_{Er} is the lifetime of the lowest excited state of Er^{3+} . The derivative of this equation gives the decay curve of Er^{3+} PL

$$I_{Er}(t) \propto N_{Si-Er}^0 \left\{ -\frac{1}{\frac{1}{\tau_R} + \frac{1}{\tau_{Tr}} + \frac{1}{\tau_{Er}}} \times \exp\left\{-\left(\frac{1}{\tau_R} + \frac{1}{\tau_{Tr}} + \frac{1}{\tau_{Er}}\right)t\right\} + \frac{1}{\tau_{Er}} \exp\left\{-\left(\frac{1}{\tau_{Er}}\right)t\right\} \right\}. \tag{10}$$

The first term of Eq. (10) expresses the increase in the intensity of the PL after pulsed excitation with the time constant $1/\tau_{rise} = 1/\tau_R + 1/\tau_{Tr} + 1/\tau_{Er}$, and the second term expresses the intensity decrease with the time constant τ_{Er} . The term τ_{Tr} can thus be estimated from τ_{rise} , τ_R and τ_{Er} .

As discussed in the previous subsection, the rising part of the decay curves could not be fitted by a single-exponential function. In this respect, Eq. (10) does not properly express the experimental data. This discrepancy seems to arise from size distributions of *nc*-Si.²⁴ Since the rise time depends on the size of *nc*-Si as clearly demonstrated in Fig.

5, the observed data are the superposition of the data from different sizes of *nc*-Si. Therefore, even if each process is expressed by a single-exponential function, the actual data should deviate from a single-exponential function.

To roughly estimate τ_{Tr} , we adopt τ_{rise} in Table I. The values of τ_R are obtained from the slopes in the tail region of the decay curves in Fig. 3(a), because the first term of Eq. (8) decays very slowly. The values of τ_{Er} can easily be estimated from decay curves. The estimated values of τ_{rise} , τ_R , τ_{Er} and τ_{Tr} are listed in Table I. We can see that τ_{Tr} becomes smaller with decreasing the size. Furthermore, τ_{Tr} is always much smaller than τ_R .

Although not shown here, the energy transfer time was almost independent of temperature. On the other hand, radiative recombination time of excitons in *nc*-Si increased with decreasing the temperature.^{24,25} Therefore, in the whole temperature range studied in this work, energy transfer is the preferential process for excitons in *nc*-Si.

It is noted here that τ_{Tr} is the sum of the energy transfer time and the time necessary to relax from the higher excited states ($^4I_{11/2}$ or $^4I_{9/2}$) of Er^{3+} to the lowest excited state ($^4I_{13/2}$). We tried to extract the relaxation time by directly exciting the third excited state ($^4I_{9/2}$). However, the time was shorter than our instrumental limit. Therefore, τ_{Tr} estimated in the above purely reflects the energy transfer time.

IV. DISCUSSION

Before discussing the observed PL properties, we summarize PL properties of bulk Si crystal and *nc*-Si not containing Er. Bulk Si crystal is an indirect gap semiconductor with the conduction band minima in the vicinity of the X points of the Brillouin zone (Δ minima). Momentum-conserving phonons thus participate in the optical transition. In general, TO phonon-assisted transition is the most dominant in the PL, and the nonphonon (NP) transition probab-

ity is negligibly small. This fundamental property of Si is preserved even for particles smaller than 10 nm. In nanometer-sized crystals, excitons are confined in a space compatible or smaller than the Bohr radius of free excitons in bulk Si crystal. This confinement increases the uncertainty of their quasimomentum, thus allowing NP optical transitions. The ratio of the NP to phonon-assisted transition is studied as a function of a confinement energy.²⁶ The ratio is estimated to be around several % for the sample with $d_{\text{Si}} = 5.5$ nm, and around several tens of % for $d_{\text{Si}} = 2.7$ nm. The increase in the NP transition rate with respect to the phonon-assisted one results in the shortening the radiative lifetime of $nc\text{-Si}$.^{24,26,27}

PL spectra under the nonresonant excitation are very broad and featureless. This inhomogeneous broadening of the PL band is mainly caused by the nanocrystal size and shape variation. The inhomogeneous broadening can be lifted by resonant PL spectroscopy; only the particles having the excitation threshold at the near-infrared laser energy are selectively excited. In pure $nc\text{-Si}$, resonant PL spectroscopy has been widely used to study the nearly homogeneous spectral shape, and some features corresponding to TO and TA momentum-conserving phonons are observed.²⁵ Similarly, by a hole burning technique, only the particles having the excitation threshold larger than the pump laser energy are selectively suppressed. The suppressed spectrum is demonstrated to coincide with the resonant PL spectrum.²⁸

The features observed in Fig. 2 can be regarded as a kind of hole burning spectroscopy. PL from $nc\text{-Si}$ with some particular sizes are suppressed by exciting Er^{3+} by the energy transfer. First we analyze the features around 1.3 eV. The positions of the features are close to the energy separation between the second excited state (${}^4I_{11/2}$) and the ground state (${}^4I_{15/2}$) of Er^{3+} ($\Delta E_{11/2-15/2} = 1.26$ eV). This suggests that the energy transfer is made to the second excited state. However, the value of $\Delta E_{11/2-15/2}$ is slightly larger than the onset of the lowest energy PL feature, i.e., the lowest energy negative peak in the derivative spectra (1.2 eV, see Fig. 2). This discrepancy can be explained by considering the indirect band gap nature of $nc\text{-Si}$. As mentioned in the above, the dominant radiative recombination process of $nc\text{-Si}$ as large as 5 nm in diameter is the TO phonon emission one. Since TO phonon energy at Δ minima [$E_{\Delta(\text{TO})}$] is 57 meV, the feature at 1.20 eV corresponds to the exciton with the recombination energy of 1.257 eV. This value agrees well with that of $\Delta E_{11/2-15/2}$. Therefore, the appearance of the dip at 1.20 eV implies that the exciton with the recombination energy of 1.257 eV recombines and resonantly excites the ${}^4I_{11/2}$ state.

The PL features appear periodically with a period of about 64 meV, which corresponds to the optical phonon energy of Si at the Γ point [$E_{\Gamma(O)}$]. This indicates that excitons with the recombination energies of $1.26 \text{ eV} + E_{\Gamma(O)} \times n$ ($n = 0, 1, 2$) can also resonantly excite Er^{3+} with the assistance of the Γ point optical phonons [$\Gamma(O)$] to satisfy the energy conservation rule. Therefore, periodic features appear at the energies of

$$1.26 \text{ eV} + E_{\Gamma(O)} \times n - E_{\Delta(\text{TO})}. \quad (11)$$

The fact that the suppression of the spectra starts at 1.2 eV

(not at 1.26 eV) implies that, in contrast to the radiative recombination of excitons, momentum conserving phonons do not participate in the energy transfer process. In other words, photoexcited excitons recombine without emitting a momentum conserving phonon and transfer the recombination energy to Er^{3+} . Only phonons in the center of the Brillouin zone can participate in the process to satisfy the energy conservation rule.

Similar to the excitation to the second excited state, that to the third excited state (${}^4I_{9/2}$) is possible. In that case, the PL features appear at

$$\Delta E_{9/2-15/2} + E_{\Gamma(O)} \times n - E_{\Delta(\text{TO})}, \quad (12)$$

where $\Delta E_{9/2-15/2}$ is the energy separation between the third excited state and the ground state. The energy position of the periodic features in Fig. 2 can be reproduced by the formula if $\Delta E_{9/2-15/2}$ is 1.53 eV, which is close to the value reported for Er-doped glasses.²⁹⁻³¹ Compared to the energy transfer to the second excited state, the PL features are ill defined. The size of particles emitting light in this region is smaller than those around 1.26 eV. The smaller size leads to the larger probability of NP recombination of excitons. This means that, in addition to the spectral positions that satisfy Eq. (12), features would appear at $\Delta E_{9/2-15/2} + E_{\Gamma(O)} \times n$. The overlap of these features and the broadening of the phonon structures by the size effects (phonon confinement effects) are considered to be responsible for the ill-defined structures.

It is worth noting that the PL spectra of $nc\text{-Si}$ become weak in a whole spectral range with increasing Er concentration, i.e., not only the spectral positions that satisfy Eqs. (11) and (12) but also other regions in broad PL bands of $nc\text{-Si}$ are quenched.^{12,13} Furthermore, the area of the observed dips was less than $\sim 1\%$ of that of Er PL at 5 K. These indicate that there is a dominant nonresonant energy transfer process in addition to the resonant one. The energy conservation rule during the energy transfer is satisfied not only by emitting $\Gamma(O)$ but also by emitting various combinations of optical and acoustic phonons with the total momentum of zero. However, the observation of clear $\Gamma(O)$ -related dips indicates that, among various processes, $\Gamma(O)$ emission one is the most dominant in the energy transfer process.

In Er-doped bulk Si crystal, the excitation of Er^{3+} is made to the first excited state (${}^4I_{15/2}$). Since the lifetime of the state is very long, the relaxation of excited Er^{3+} by the phonon-assisted re-excitation of host Si (energy back transfer) is possible at relatively high temperatures and is one of the major nonradiative relaxation processes at room temperature. In the present samples, excitation of Er^{3+} is made to the second or third excited states due to the large band gap. Er^{3+} excited to these higher states is considered to relax promptly to the lowest excited state (${}^4I_{13/2}$) before the energy back transfer occurs. The probability of the back transfer from the lowest excited state to $nc\text{-Si}$ is negligibly small even at room temperature due to the large energy mismatch. This may result in the extremely small temperature quenching of the PL observed previously.¹²

Free excitons in bulk Si crystal cannot recombine without emitting/absorbing momentum-conserving phonons due to its indirect band gap nature. In the case of Er-doped bulk

Si crystal, recombination energy of free excitons is not directly transferred to Er^{3+} , but the energy transfer is mediated by Er-related trap centers.⁵⁻⁸ An exciton generated in Si is first trapped at an Er-related level about 0.15 eV below the bottom of the conduction band. The localization of an exciton in a small space partially breaks the momentum conservation rule and makes the direct recombination of the exciton possible. The recombination energy of the trapped exciton is then transferred to Er^{3+} , and the $4f$ shell is excited.

In contrast to Er-doped bulk Si crystal, the existence of such a trap level is not experimentally shown in the present samples and also in Er-doped porous Si. In the present samples, Er^{3+} responsible for energy transfer are considered to be not doped in nc -Si, but exist in the vicinity of nc -Si.^{17,19} Therefore, it might be possible that energy transfer is not mediated by Er-related trap states. Under this assumption, we propose the following model to explain the size dependence of the energy transfer rate.

As mentioned in the above, NP recombination of free excitons is partially allowed in nanocrystals, although for nc -Si exhibiting PL at around 1.2 eV, the probability of NP transition is much smaller than that of the phonon-assisted one because of the relatively large size and resulting weak confinement. Similarly, the energy transfer is considered to be restricted by the momentum conservation rule and the rate is small. As the size decreases, the overlap of the electron and hole wave functions becomes larger. This may increase the probability of the NP radiative recombination as well as the energy transfer rate. We believe that the energy transfer rate is mainly determined by the degree of the breakdown of the k -conservation rule during the optical transition in nc -Si induced by the quantum confinement effects.

The probability of the quasidirect recombination of excitons in nc -Si depends not only on the size but also on the crystallinity. A disorder in the translation invariance of the crystalline lattice brings about a breakdown of the k -conservation rule, and makes the probability of NP transition large. It seems to be very interesting to study the effects of disorder on the energy transfer rate.

V. CONCLUSION

The present results demonstrate the first spectroscopic evidence of the strong coupling between nc -Si and Er^{3+} . The observation of phonon-related periodic features in broad nc -Si PL band is the direct evidence of the existence of resonant energy transfer processes. The observed periodic features indicate that excitons in nc -Si interact with the second or third excited states of Er^{3+} . We also observed a delay of Er^{3+} PL after the pulsed excitation of host nc -Si. From the observed size dependence of the delay time, it is found that the smaller the nc -Si, the larger the energy transfer rate.

The present results strongly suggest that two major aspects of the quantum size effects of nc -Si, i.e., widening of the band gap and the increase in the quasidirect recombination of excitons, play crucial roles for the efficient luminescence of Er^{3+} . The excitation to the higher excited states and the prompt relaxation to the first excited state make the en-

ergy back transfer process small, resulting in the small temperature quenching of the PL. Furthermore, the increase in the uncertainty in the crystal momentum relaxes the momentum conservation rule during the energy transfer process and realizes the higher energy transfer rate.

ACKNOWLEDGMENTS

The authors are grateful to Hiroyuki Tamaoka for his valuable assistance in this work. This work was supported by a Grant-in-Aid for Science Research from the Ministry of Education, Science and Culture, Japan, and a Grant for Research for the Future Program from the Japan Society for the Promotion of Science (JSPS-RFTF-98P-0120). One of authors (K.W.) would like to thank the Japan Society for the Promotion of Science for financial support.

- ¹S. Lombardo, S. U. Campisano, G. N. van den Hoven, and A. Polman, *J. Appl. Phys.* **77**, 6504 (1995).
- ²J. Stimmer, A. Reittinger, J. F. Nützel, G. Abstreiter, H. Holzbrecher, and Ch. Buchal, *Appl. Phys. Lett.* **68**, 3290 (1996).
- ³S. Coffa, G. Franzò, and F. Priolo, *Appl. Phys. Lett.* **69**, 2077 (1996).
- ⁴G. Franzò, S. Coffa, F. Priolo, and C. Spinella, *J. Appl. Phys.* **81**, 2784 (1997).
- ⁵A. Polman, *J. Appl. Phys.* **82**, 1 (1997).
- ⁶F. Priolo, G. Franzò, S. Coffa, and A. Carnera, *Phys. Rev. B* **57**, 4443 (1998).
- ⁷A. Taguchi and K. Takahei, *J. Appl. Phys.* **83**, 2800 (1998).
- ⁸A. Taguchi, K. Takahei, M. Matsuoka, and S. Tohno, *J. Appl. Phys.* **84**, 4471 (1998).
- ⁹J. H. Shin, G. N. van den Hoven, and A. Polman, *Appl. Phys. Lett.* **66**, 2379 (1995).
- ¹⁰S. Seo and J. H. Shin, *Appl. Phys. Lett.* **75**, 4070 (1999).
- ¹¹U. Hömmerich, F. Namavar, A. Cremins, and K. L. Bray, *Appl. Phys. Lett.* **68**, 1951 (1996).
- ¹²M. Fujii, M. Yoshida, S. Hayashi, and K. Yamamoto, *J. Appl. Phys.* **84**, 4525 (1998).
- ¹³M. Fujii, M. Yoshida, S. Hayashi, and K. Yamamoto, *Appl. Phys. Lett.* **71**, 1198 (1997).
- ¹⁴K. Watanabe, M. Fujii, and S. Hayashi, *J. Lumin.* **87-89**, 426 (2000).
- ¹⁵C. E. Chrissy, A. J. Kenyon, T. S. Iwayama, C. W. Pitt, and D. E. Hole, *Appl. Phys. Lett.* **75**, 2011 (1999).
- ¹⁶P. G. Kik, M. L. Brongersma, and A. Polman, *Appl. Phys. Lett.* **76**, 2325 (2000).
- ¹⁷P. G. Kik and A. Polman, *J. Appl. Phys.* **88**, 1992 (2000).
- ¹⁸G. Franzò, V. Vinciguerra, and F. Priolo, *Appl. Phys. A: Mater. Sci. Process.* **69**, 3 (1999).
- ¹⁹G. Franzò, D. Pacifici, V. Vinciguerra, and F. Priolo, *Appl. Phys. Lett.* **76**, 2167 (2000).
- ²⁰G. Qin, G. G. Qin, and S. H. Wang, *J. Appl. Phys.* **85**, 6738 (1999).
- ²¹Y. Kanzawa, T. Kageyama, S. Takeoka, M. Fujii, S. Hayashi, and K. Yamamoto, *Solid State Commun.* **102**, 533 (1997).
- ²²H. E. Roman and L. Pavesi, *J. Phys.: Condens. Matter* **8**, 5161 (1996).
- ²³D. T. X. Thao, C. A. J. Ammerlaan, and T. Gregorkiewicz, *J. Appl. Phys.* **88**, 1443 (2000).
- ²⁴S. Takeoka, M. Fujii, and S. Hayashi, *Phys. Rev. B* **62**, 16820 (2000).
- ²⁵D. Kovalev, H. Heckler, G. Polisski, and F. Koch, *Phys. Status Solidi B* **215**, 871 (1999).
- ²⁶D. Kovalev, H. Heckler, M. Ben-Chorin, G. Polisski, M. Schwartzkopff, and F. Koch, *Phys. Rev. Lett.* **81**, 2803 (1998).
- ²⁷M. Fujii, D. Kovalev, J. Diener, F. Koch, S. Takaoka, and S. Hayashi, *J. Appl. Phys.* **88**, 5772 (2000).
- ²⁸D. Kovalev, H. Heckler, B. Averboukh, M. Ben-Chorin, M. Schwartzkopff, and F. Koch, *Phys. Rev. B* **57**, 3741 (1998).
- ²⁹P. E.-A. Moberg, E. Heumann, G. Huber, and B. H. T. Chai, *Appl. Phys. Lett.* **73**, 139 (1998).
- ³⁰R. Burlot-Loison, J.-L. Doualan, P. Le Boulanger, T. P. J. Han, H. G. Gallagher, R. Moncorge, and G. Boulon, *J. Appl. Phys.* **85**, 4165 (1999).
- ³¹S. Ramachandran and S. G. Bishop, *Appl. Phys. Lett.* **73**, 3196 (1998).